

Supporting information

Synthesis of ultrafine AuPd bimetallic nanoparticles using magnetite cored poly(propyleneimine) dendrimer template and its sustainable catalysis of Suzuki coupling reaction

Rajmohan Rangasamy*, Kannappan Lakshmi

Department of Chemistry, Guru Nanak College (Autonomous), Affiliated to University of Madras, Velachery, Chennai, India- 600042

Corresponding author email address- rangagncchem@gmail.com;
rangasamy.r@gurunanakcollege.edu.in

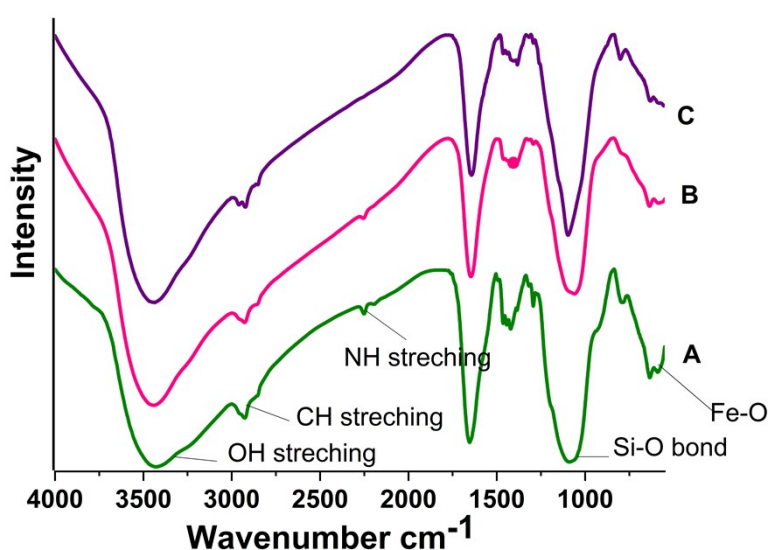


Figure S1: FTIR Spectrum for (A) PPI@Fe₃O₄/SiO₂ (B) Fresh AuPd@PPI@Fe₃O₄/SiO₂ (C) Recycled AuPd@PPI@Fe₃O₄/SiO₂

Table S1: Percentage composition of elements obtained from EDS

Element	Absorption corrections	Wt %
C	1.00	24.91
N	1.00	2.86
O	1.00	33.54
Si	1.00	21.35
Fe	1.00	11.50
Pd	1.00	3.13
Au	1.00	2.71
Total		100.00

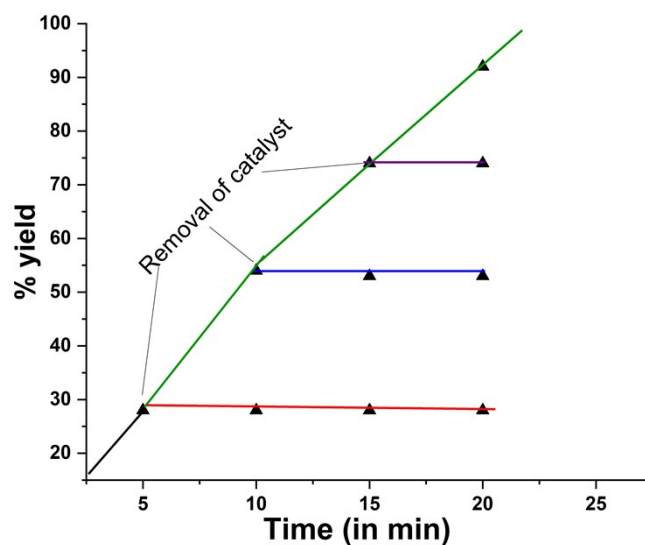


Figure S2: Hot filtration test for leaching studies of AuPd@PPI@Fe₃O₄/SiO₂ nanomaterial

XPS also evidence the carbon and nitrogen in the nanomaterial. The deconvoluted peaks were fitted into three components for carbon. C-C bond with binding energy 282.1 eV (80.8%), C-N with binding energy 284.04 eV (15.28%) and C-N bond with binding energy 290.38 eV (3.91%). Similarly, deconvoluted peaks for nitrogen were fitted into three components. C-N bond, and N-H bond C-N-C bond with binding energies 396.96 eV (72.12%), 398.02 eV (17.44%) and 399.3 (10.4 %) respectively

Table S2: Percentage composition of elements obtained from XPS Survey scan of AuPd@PPI@Fe₃O₄/SiO₂ nanomaterial

S.No.	Element	Binding Energy (in eV)	% of Atomic concentration
1	Carbon	283.4	40.28
2	Nitrogen	398	5.24
3	Iron	688.6	5.74
4	Silica	150.7	13.48
5	Oxygen	548.8	34.25
6	Gold	332.8	0.56
7	Palladium	81.07	0.45

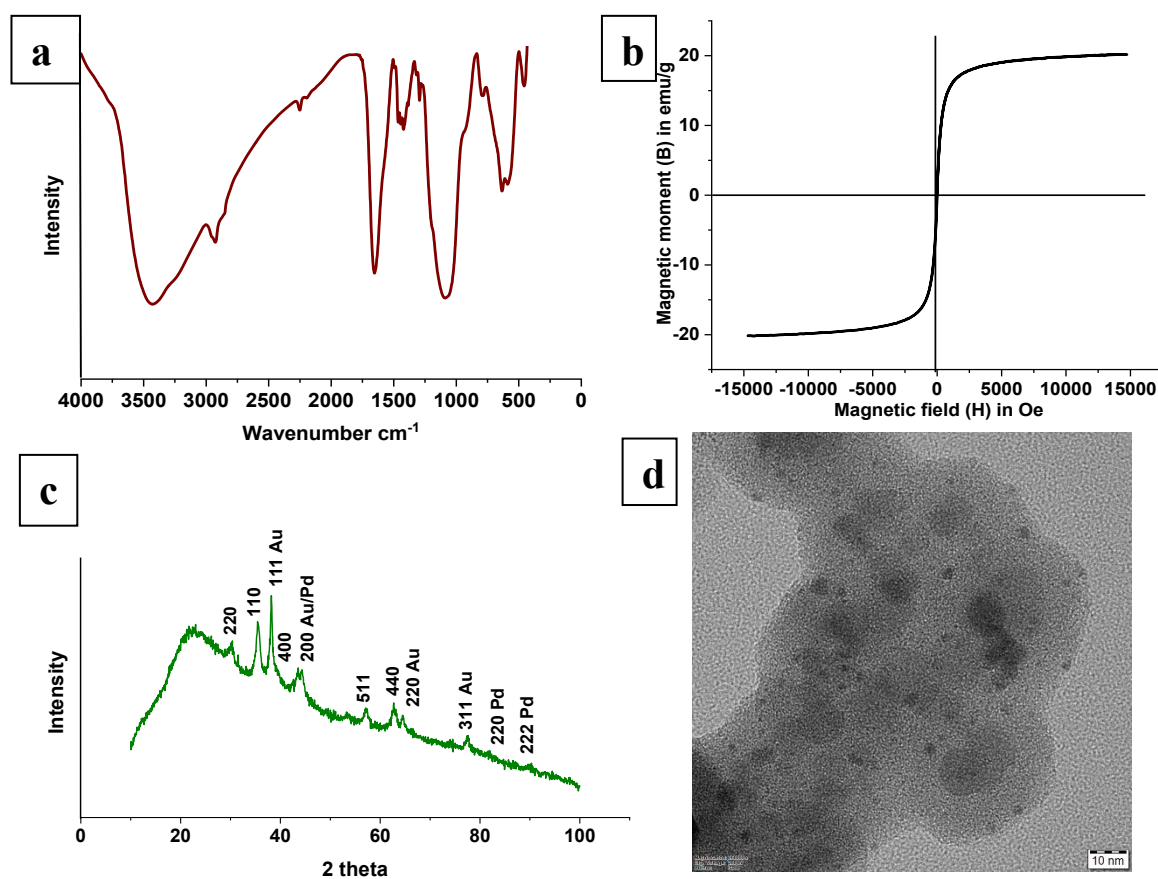


Figure S3: Recycled catalyst AuPd@PPI@Fe₃O₄/SiO₂ nanomaterial (a) FTIR spectrum (b) VSM analysis (c) XRD pattern (d) HRTEM image

The characterisation of recycled catalyst AuPd@PPI@Fe₃O₄/SiO₂ nanomaterial proves that the catalyst remains unaltered in size, shape and chemical composition. FTIR spectrum of recycled AuPd@PPI@Fe₃O₄/SiO₂ nanomaterial is similar to the fresh AuPd@PPI@Fe₃O₄/SiO₂ nanomaterial (Figure S3 a). VSM analysis proves that magnetic behaviour is retained even after recycling and it was found that magnetisation value is 20.2 emu/g which is almost equal to 20.1 emu/g for fresh catalyst (Figure S3 b). The XRD peaks obtained for the recycled catalyst AuPd@PPI@Fe₃O₄/SiO₂ nanomaterial remains unchanged proving the crystalline structure of both the nanoparticles Au and Pd, magnetite nanoparticle (Figure S3 c). Moreover, HRTEM image of the recycled AuPd@PPI@Fe₃O₄/SiO₂ nanomaterial proves the presence of AuPd bimetallic without leaching after recycled experiments (Figure S3 d).

NMR spectroscopic data of the products (Table 2)

1. **Biphenyl (Table 2, entry 1)**, $C_{12}H_{10}$ ¹⁻ ¹H NMR (400 MHz, CDCl₃); δ (ppm), 7.57 (dd, J=12.0 Hz, 4.0 Hz, 4H), 7.42 (t, J=10.0 Hz, 4H), 7.32 (t, J=12.0 Hz, 2H); ¹³C NMR (100 MHz, CDCl₃); δ (ppm) 140.3, 127.7, 126.5, 126.1
2. **4-phenyl anisole (Table 2, entry 2-5, 14, 15)**, $C_{13}H_{12}O$ ¹⁻ ¹H NMR (400 MHz, CDCl₃); δ (ppm) 7.56 (m, 4H), 7.40 (t, J=8.0 Hz, 2H), 7.31 (tt, J=8.0 Hz, 1H), 6.99 (d, J=10.0 Hz, 2H), 3.89 (s, 3H); ¹³C NMR (100 MHz, CDCl₃); δ (ppm) 163.2, 137.5, 135.3, 127.7, 114.1, 113.6, 113.5, 55.19
3. **4,4'-dimethoxy-1,1'-biphenyl (Table 2, entry 6)**, $C_{14}H_{14}O_2$ ²⁻ ¹H NMR (400 MHz, CDCl₃); δ (ppm) 8.18 (d J=8.0 Hz, 2H), 7.70, (m, 4H), 7.02 (m, 4H), 3.83 (s, 6H); ¹³C NMR (100 MHz, CDCl₃); δ (ppm) 163.2, 137.5, 135.3, 127.7, 114.1, 113.6, 113.5, 55.19
4. **4-acetyl 4'-methoxy 1,1'-biphenyl (Table 2, entry 8)**, $C_{15}H_{14}O_2$ ³⁻ ¹H NMR (400 MHz, CDCl₃); δ (ppm) 7.95 (d, J= 8.0 Hz, 2H), 7.65 (d, J= 8.0 Hz, 2H), 7.52 (d, J= 8.0 Hz, 2H), 6.94 (d, J= 8.0 Hz, 2H), 3.87 (s, 3H), 2.56 (s, 3H); ¹³C NMR (100 MHz, CDCl₃); δ (ppm) 198, 159.9, 145.4, 135.3, 132.2, 128.9, 128.3, 126.6, 114.4, 55.4, 26.62
5. **1,1'-biphenyl 4-carboxamide (Table 2, entry 9)**, $C_{13}H_{11}NO$ ⁴⁻ ¹H NMR (400 MHz, CDCl₃); δ (ppm) 10.02 (s, 2H), 7.83 (d, J= 8.0 Hz, 2H), 7.62 (d, J= 8.0 Hz, 2H), 7.56 (d, J= 8.0 Hz, 2H), 7.42 (d, J= 8.0 Hz, 1H), 7.35 (d, J= 8.0 Hz, 2H) ; ¹³C NMR (100 MHz, CDCl₃); δ (ppm) 162.8, 159.3, 128.9, 128.1, 127.9, 127.3, 127.2, 113.2, 55.2
6. **4-phenyl benzaldehyde (Table 2, entry 10,12)**, $C_{13}H_{10}O$ ⁵⁻ ¹H NMR (400 MHz, CDCl₃); δ (ppm) 10.08 (s, 1H), 8.00 (tt, J= 12.0 Hz, 1.5 Hz 2H), 7.80 (dd, J= 12.0 Hz, 2 Hz 2H), 7.65 (d, J=8 Hz, 2H), 7.54 (m, 2H), 7.39 (tt, J= 7.0 Hz, 1.0 Hz 1H); ¹³C NMR (100 MHz, CDCl₃); δ (ppm) 192.0, 145.5, 135.9, 133.6, 130.4, 129.0, 128.1, 128.0, 127.7, 127.3
7. **4'-methoxy 4-phenyl benzaldehyde (Table 2, entry 11,13)**, $C_{14}H_{12}O_2$ ⁵⁻ ¹H NMR (400 MHz, CDCl₃); δ (ppm) 10.02 (s, 1H), 8.18 (d, J= 8.0 Hz, 1H), 7.70 (m, 1H), 7.48 (d, J=10.0 Hz, 2H), 7.29 (m, 2H), 7.02 (d, J= 8.0 Hz, 2H), 3.89 (s, 3H); ¹³C NMR (100

MHz, CDCl₃); δ (ppm) 163.2, 158.6, 137.5, 135.3, 133.5, 127.7, 114.18, 113.6, 113.5, 55.36, 55.14, 29.7

8. **9-(4-methoxyphenyl)-anthracene (Table 2, entry 16), C₂₁H₁₆O** ⁶. ¹H NMR (400 MHz, CDCl₃); δ (ppm) 8.06 (s, 4H), 7.60 (d, J= 4.0 Hz, 4H), 7.35 (s, 2H), 7.13 (s, 1H), 6.96 (s, 2H), 3.84 (m, 3H); ¹³C NMR (100 MHz, CDCl₃); δ (ppm) 131.1, 129.5, 127.5, 127.3, 126.6, 126.1, 126.0, 125.8, 124.6, 121.3, 113.1, 112.7, 54.3
9. **2-phenyl naphthalene (Table 2, entry 17), C₁₆H₁₂** ⁷. ¹H NMR (400 MHz, CDCl₃); δ (ppm) 7.99 (s, 1H), 7.87 (m, 3H), 7.71 (t, J=12.0 Hz, 3H), 7.56 (t, J=12.0 Hz, 4H), 7.5 (t, J=12.0 Hz, 1H); ¹³C NMR (100 MHz, CDCl₃); δ (ppm) 141.1, 138.5, 133.7, 132.6, 128.8, 128.4, 128.2, 127.4, 127.6, 127.3, 126.3, 125.9, 125.8, 125.6
10. **2-(4-methoxyphenyl) naphthalene (Table 2, entry 18), C₁₇H₁₄O** ⁷. ¹H NMR (400 MHz, CDCl₃); δ (ppm) 8.1 (s, 1H), 7.92 (t, J=10.0 Hz, 2H), 7.84 (d, J=8.0 Hz, 2H), 7.73 (t, J=12.0 Hz, 2H), 7.71 (m, 2H), 7.62 (d, J= 8.0 Hz, 2H), 7.47 (m, 2H), 7.28 (t, J=12.0 Hz, 1H); ¹³C NMR (100 MHz, CDCl₃); δ (ppm) 138.4, 137.9, 133.7, 132.6, 128.5, 128.2, 127.9, 126.5, 126.3, 125.7, 123.6, 109.4, 55.2

Characterization

High Resolution Transmission Electron Microscopy (HRTEM) microscopic images were taken in High Resolution Transmission Electron Microscope, JEOL Japan JEM 2100 at 200 KV model with LaB6 electron gun. About 0.1 mg AuPd@PPI@Fe₃O₄/SiO₂ nanomaterial was dispersed in 1mL of ethanol and sonicated; a representative μ L of this solution was placed on the carbon coated mesh on copper grid and dried for an hour. The grid was placed under electron beam and images were captured.

X-ray Photoelectron Spectroscopy was carried with AES Module with Ar ion as well as C60 sputter Guns, PHI 5000 Versa Probe II, FEI Inc. Operating in a mode analogous to a rotating anode, a high power (100 W) 100 μ m diameter X-ray beam is scanned 1.4 mm in the non-dispersive direction of the x-ray monochromator at high speed, providing a large rectangular analysis area with both high sensitivity and high energy resolution.

X-ray Diffraction Patterns were recorded in Bruker USA D8 Advance, Davinci using CuK α radiations with wavelength 0.1541 nm. The measurements were made between the angles 10 $^\circ$ and 70 $^\circ$. The FWHM was determined for 311 lattice plane and the crystallite size of the magnetite nanoparticle was calculated from the Scherrer equation $D = (K \cdot \lambda) / (\beta \cdot \cos \theta)$ where $K = 0.69$, $\lambda =$ wavelength of X-Ray, $\beta =$ FWHM

Magnetic behaviour of the nanohybrid materials synthesized were analysed by using Vibrating Sample Magnetometer Lakeshore, 7410 series with a maximum field of 3.1 Tesla at room temperature having field setting resolution of 30 mOe.

FTIR spectra was obtained from Perkin Elmer instrument in transmittance mode for measurements in the range of 4100- 400 cm^{-1} using KBr pellets sampling method.

^1H and ^{13}C NMR were recorded FT NMR Spectrometer model Avance-II (Bruker). The instrument is equipped with a cryomagnet of field strength 9.4 T. Its ^1H frequency is 400 MHz, while for ^{13}C the frequency is 100 MHz.

References

- 1 G. Zhang, Y. Luan, X. Han, Y. Wang, X. Wen, C. Ding and J. Gao, *Green Chem.*, 2013, **15**, 2081–2085.
- 2 S. Dwivedi, S. Bardhan, P. Ghosh and S. Das, *RSC Adv.*, 2014, **4**, 41045–41050.
- 3 S. L. Mao, Y. Sun, G. A. Yu, C. Zhao, Z. J. Han, J. Yuan, X. Zhu, Q. Yang and S. H. Liu, *Org. Biomol. Chem.*, 2012, **10**, 9410–9417.
- 4 X. Guo, L. Tang, Y. Yang, Z. Zha and Z. Wang, *Green Chem.*, 2014, **16**, 2443–2447.
- 5 R. Singha, S. Dhara, M. Ghosh and J. K. Ray, *RSC Adv.*, 2015, **5**, 8801–8805.
- 6 V. M. Zende, C. Schulzke and A. R. Kapdi, *Org. Chem. Front.*, 2015, **2**, 1397–1410.
- 7 B. Wen-Juan Shi, a Xiao-Lei Li, a Zhao-Wei Li a and Zhang-Jie Shi a, *Org. Chem. Front.*, 2016, **3**, 375–379.